International Journal of Solids and Structures 47 (2010) 2893–2904

Contents lists available at ScienceDirect

International Journal of Solids and Structures

journal homepage: www.elsevier.com/locate/ijsolstr

Piezoelectric composites with periodic multi-coated inhomogeneities

R. Hashemi [a], G.J. Weng [b,*], M.H. Kargarnovin [a], H.M. Shodja [c]

[a] Department of Mechanical Engineering, Sharif University of Technology, Tehran, Iran
[b] Department of Mechanical and Aerospace Engineering, Rutgers University, New Brunswick, NJ 08903, USA
[c] Department of Civil Engineering, Sharif University of Technology, Tehran, Iran

ARTICLE INFO

Article history:
Received 20 December 2009
Received in revised form 30 May 2010
Available online 25 June 2010

Keywords:
Piezocomposite
Periodic structure
Multi-coated particulates
Equivalent inclusions
Micromechanics
Homogenization

ABSTRACT

A new, robust homogenization scheme for determination of the effective properties of a periodic piezoelectric composite with general multi-coated inhomogeneities is developed. In this scheme the coating does not have to be thin, the shape and orientation of the inclusion and coatings do not have to be identical, their centers do not have to coincide, their properties do not have to remain uniform, and the microstructure can be with the 2D elliptic or the 3D ellipsoidal inclusions. The development starts from the local electromechanical equivalent inclusion principle through the introduction of the position-dependent equivalent eigenstrain and electric field. Then with a Fourier series expansion and a superposition procedure, the volume-averaged equivalent eigenstrain and electric field for each phase are obtained. The results in turn are used in an energy equivalent criterion to determine the effective properties of the composite. In this model the interphase interactions in each multi-coated particle and the long-range interactions between the periodically distributed particles are fully accounted for. To demonstrate its wide range of applicability, we applied it to examine the properties of several periodic composites: (i) piezoelectric PZT spherical particles in a polymer matrix, (ii) continuous glassy fibers with thin PZT coating in an epoxy matrix, (iii) spherical PZT particles coated by thick or functionally graded piezoelectric layer, (iv) spheroidal voids coated with a thick non-piezoelectric layer in a PZT matrix, and (v) spherical piezoelectric inhomogeneities with eccentric, non-uniform thickness coating. The calculated results reflect the complex nature of interplay between the properties of core, matrix, and coating, as well as whether the coating is uniform, functionally graded, or eccentric. The accuracy of this new scheme is checked against the double-inclusion and other micromechanics models, and good agreement is observed.

1. Introduction

The coupling behavior of a piezoelectric composite is a key factor for its applications in smart materials and structures, such as electromechanical transducers, sensors, actuators and micro generators. Hence the problem of a piezoelectric material embedded in an elastic medium or vice versa, and that of a piezoelectric material containing defects or voids, have received considerable attention in recent past. Most contributions in the literature are concerned with the determination of the overall behavior of conventional two-phase piezoelectric composites (e.g. Dunn and Taya, 1993; Huang, 1995; Wu, 2000; Fang et al., 2001; Wei et al., 2006). These studies have revealed the significance of a piezoelectric inclusion phase on the electromechanical coupling of an otherwise non-piezoelectric polymer matrix.

The improvement of electromechanical coupling greatly depends on the load transfer condition from the matrix to the inhomogeneities. As a result the bond quality between the two can play a very significant role. To improve the bonding strength, the piezoelectric reinforcements are often coated by an elastic layer. This coating can prevent the premature fracture of reinforcements, the initiation of interfacial cracks, or the development of large residual stress during the cool-down process. On the other hand it has also been observed that piezoelectric inhomogeneities with non-piezoelectric core can have other advantage over the conventional two-phase composites. With glassy reinforcements surrounded by a thin layer of PZT coating, Beckert et al. (2001) have shown that substantial improvement in the electromechanical properties of a polymer matrix composite can be attained.

Recognizing the potential gain that coated inhomogeneities could deliver, some investigators have paid special attention to this topic. Li (2000) has extended the double-inclusion theory of Hori and Nemat-Nasser (1993, 1994) to magnetoelectroelastic composites. In the elastic context, the double-inclusion theory has been applied by Dunn and Ledbetter (1995) to develop a micromechanical theory with coated inclusions with experimental verification, and it has been shown by Hu and Weng (2000) to have wide

* Corresponding author. Tel./fax: +1 732 445 3124.
E-mail address: weng@jove.rutgers.edu (G.J. Weng).

0020-7683/$ - see front matter © 2010 Elsevier Ltd. All rights reserved.
doi:10.1016/j.ijsolstr.2010.06.017

connection with a number of existing homogenization theories. Other exact analyses in the elastic context can also be found in Christensen and Lo (1979), and Qiu and Weng (1991). Li's treatment has served as a basis for the development of an averaging scheme for composite materials with magnetoelectroelastic multi-inhomogeneities. Jiang and Cheung (2001) and Jiang et al. (2001) have derived the local electroelastic fields in coated long fibers. Based on their solution, some existing averaging models have been extended to predict the electroelastic moduli of fibrous piezoelectric composites. Sudak (2003) and Shen et al. (2005) have examined the influence of an interphase layer and a confocally multi-coated elliptic inclusion, respectively, under remote loading. Both studies made use of the complex variable approach, and are two-dimensional. Dinzart and Sabar (2009) have applied the Mori–Tanaka method to calculate the effective properties of a piezoelectric composite containing thinly coated inhomogeneities. More recently, using the well-known double-inclusion model, Lin and Sodano (2010) have performed a homogenizing study on a piezocomposite system containing coated circular cylinders, and found their results to be in excellent agreement with the finite element analysis. All of these studies are pertinent to the randomly distributed coated reinforcements or to a single-inclusion problem; none was concerned with a periodic structure. Composites with a periodic structure of course have been studied extensively in the elastic context (Nemat-Nasser et al., 1993; Nemat-Nasser and Hori, 1999) and, with the exception of a recent one on electrostrictive material without coating (Yu and Somphone, 2009), we have not seen any studies that address the electroelastic properties of a periodic, multi-coated piezoelectric composite.

This is the intent of this study. We will start from the electromechanical equivalent inclusion principle to estimate the local electromechanical field, and then integrate it over the phase volume to obtain the average equivalent eigenstrain-electric field of each phase. The periodic microstructure will be accounted for through a Fourier series expansion. We will then call upon the energy equivalence between a homogeneous effective medium and the heterogeneous periodic structure to evaluate the effective electroelastic moduli of the piezoelectric composite. Here the micromechanical configuration of a typical multi-coated inhomogeneity system is composed of an ellipsoidal inhomogeneity surrounded by many layers of coatings of ellipsoidal shape. The coatings do not have to be thin, their shapes do not have to be identical, their orientations do not have to be aligned, their origins do not have to coincide, and the property of a layer can be functionally graded. As such, the morphology of the composite is sufficiently general, and the developed methodology can be quite robust to handle a variety of problems. A typical configuration of such a multi-coated inhomogeneity system is depicted in Fig. 1. This system is to be distributed periodically in the matrix, to form a periodic composite.

2. Problem statement and basic notations

Consider an infinitely extended piezoelectric body Φ which contains periodically distributed piezoelectric multi-inhomogeneities of common geometry and dimensions. A typical reinforcement particle as shown in Fig. 1 is made of an inner ellipsoidal inhomogeneity, $\psi_1 \equiv \Omega_1$, which is surrounded by an arbitrary number of coating layers, Ω_α, $\alpha = 2,3,\ldots,N$. The sequence, $\psi_1, \psi_2, \ldots, \psi_N = \bigcup_{\alpha=1}^{N} \Omega_\alpha$, then forms a set of nested ellipsoidal multi-inhomogeneities. The tensors of elastic, piezoelectric and dielectric properties of the unbounded matrix are denoted by C_{ijkl}, e_{ijk} and K_{ij}, respectively, whereas the properties of all other phases are differentiated with a corresponding superscript, Ω_α, $\alpha = 1,2,\ldots,N$. The far-field displacement and electric potential prescribed on the boundary are given by $u_i^o = \varepsilon_{ij}^o x_j$ and $\phi^o = -E_i^o x_i$, to give rise to an uniform overall strain and electric field, denoted as ε_{ij}^o and E_i^o, respectively.

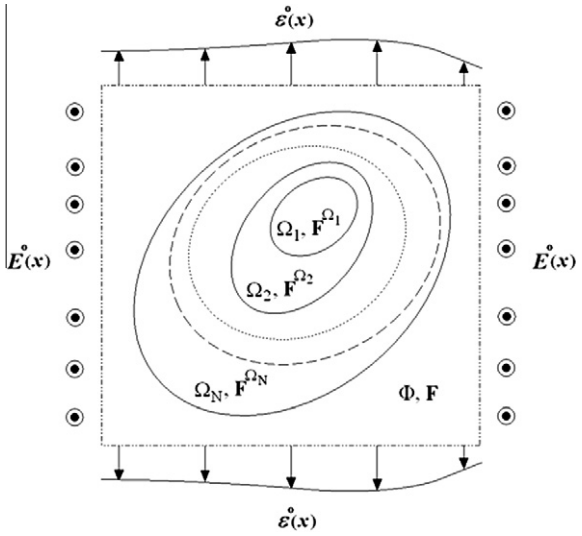

Fig. 1. A typical multi-coated ellipsoidal inhomogeneity contained in a representative volume element of a piezocomposite.

In the analysis we shall adopt the notations introduced by Barnett and Lothe (1975) so that all the electromechanical moduli can be written in an unified fashion. Herein the lowercase subscripts range from 1 to 3, and the uppercase ones range from 1 to 4, with the subscript 4 referring to the piezoelectric quantities. Accordingly the field variables of the material take the following shorthand forms:

$$\Sigma_{iJ} = \begin{cases} \sigma_{ij}, & J = 1,2,3, \\ D_i, & J = 4, \end{cases} \quad U_J = \begin{cases} u_J, & J = 1,2,3, \\ \phi, & J = 4, \end{cases} \quad Z_{Mn} = \begin{cases} \varepsilon_{Mn}, & M = 1,2,3, \\ -E_n, & M = 4, \end{cases} \tag{1}$$

for the pairs of stress and electric displacement, mechanical displacement and electric potential, and strain and electric field, respectively. In a similar manner the electroelastic moduli are expressed as

$$F_{iJMn} = \begin{cases} C_{ijmn}, & J,M = 1,2,3, \\ e_{nij}, & J = 1,2,3, M = 4, \\ e_{imn}, & J = 4, M = 1,2,3, \\ -K_{in}, & J,M = 4. \end{cases} \tag{2}$$

With this set off notations the linear constitutive relation can be written as

$$\Sigma_{iJ} = F_{iJMn} Z_{Mn}. \tag{3}$$

3. Average eigenstrain-electric field in periodically distributed multi-inhomogeneities

Following Eshelby's equivalent inclusion principle (Eshelby, 1957) but written for a piezoelectric medium, we now replace the multi-inhomogeneities that carry different moduli with the equivalent multi-inclusions with the properties of the matrix but carrying certain equivalent eigenstrain and electric field, denoted by a starred quantity, $Z_{Mn}^{*(\Omega_\alpha)}(x)$. The magnitude of $Z_{Mn}^{*(\Omega_\alpha)}(x)$ is determined on the basis that the fields in the original heterogeneous system and in the equivalent homogeneous system but carrying this specified eigenfield would be identical. Due to the complex nature of the microgeometry, this quantity is position-dependent. Such a configuration is shown in Fig. 2. This equivalency holds for a proper choice of $Z_{Mn}^{*(\Omega_\alpha)}(x)$ defined over region Ω_α, $\alpha = 1,2,\ldots,N$. Since the multi-inhomogeneities have a periodic dis-

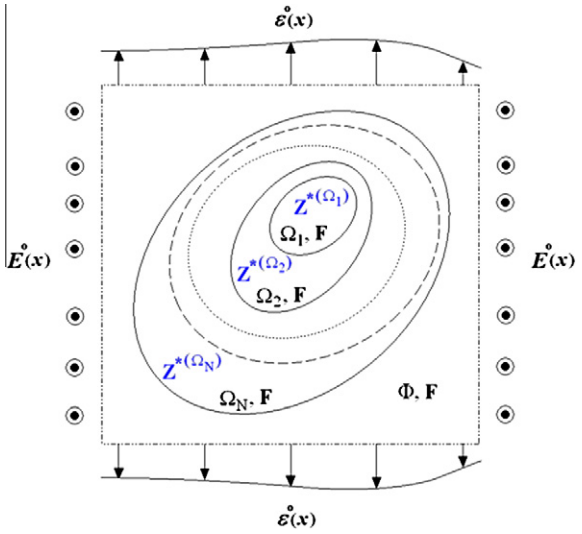

Fig. 2. Piezoelectric multi-coated inhomogeneity is replaced by an equivalent multi-inclusion with proper equivalent eigenstrain-electric field distribution.

tribution, the associated equivalent eigenstrain-electric field can be expressed in terms of the Fourier series expansion, as

$$Z^{*(\Omega_\alpha)}_{Mn}(\boldsymbol{x}) = \sum_{\xi} \widetilde{Z}^{*(\Omega_\alpha)}_{Mn}(\xi) e^{i\xi\cdot x}, \tag{4}$$

where $i = \sqrt{-1}$ and Σ is, in general, a triple summation corresponding to ξ_i, $i = 1, 2, 3$, which are in turn associated with the periodicity of the eigenstrain-electric field in the directions x_i, $i = 1, 2, 3$. On the other hand the Fourier inversion gives

$$\widetilde{Z}^{*(\Omega_\alpha)}_{Mn}(\xi) = \frac{1}{V}\int_D Z^{*(\Omega_\alpha)}_{Mn}(\boldsymbol{x}) e^{-i\xi\cdot x} dx, \tag{5}$$

in which D is the parallelepiped unit cell, periodically distributed throughout the entire domain. The volume, V of the representative volume element (RVE), D, is

$$V = \Lambda_1\Lambda_2\Lambda_3, \tag{6}$$

where Λ_i, $i = 1, 2, 3$ are the dimensions of D, measured along the respective x_i-coordinates.

We now decompose the multi-inclusion into a series of single-inclusion problems by means of a superposition scheme, in which the eigenfield of each phase is first introduced into itself, and then that of the kth phase is introduced into the $(k-1)$th region for subtraction. As we count the phase outward so that the inner inclusion is phase 1, this introduction of the eigenfield actually starts from the outermost phase. The schematic representation of such a decomposition of multi-inhomogeneity in an infinite domain under the far-field loading, Z^o_{Mn}, is illustrated in Fig. 3, where the top four figures indicate the introduction of their own eigenfield and the bottom two with a minus sign reflect the subtraction of eigenfield from its immediate outer layer. These eigenfields, $Z^{*(\gamma)}_{Mn}$, $\gamma \equiv \Omega_i$, $i = 1, 2, \ldots, N$, distributed over the single-inclusion regions, $\beta \equiv \psi_j$, $j = 1, 2, \ldots, N$, in turn produces a disturbed electroelastic field, to be denoted by $Z^d_{Mn}\left(\boldsymbol{x}; \boldsymbol{Z}^{*(\gamma,\beta)}\right)$, in the entire body which carries the properties of the matrix, F_{ijMn}. In this way the electroelastic field inside the pertinent single-inclusion can be written as

$$\Sigma_{ij}(\boldsymbol{x}) = F_{ijMn}\left[Z^o_{Mn} + Z^d_{Mn}\left(\boldsymbol{x}; \boldsymbol{Z}^{*(\gamma,\beta)}\right) - Z^{*(\gamma)}_{Mn}(\boldsymbol{x})\right], \quad \boldsymbol{x} \in \beta. \tag{7}$$

The stress and electric displacement must satisfy the electromechanical equilibrium equations, $\Sigma_{ij,i} = 0$. Since the prescribed far-field Z^o_{Mn} is uniform, it implies that

$$F_{ijMn}\left[Z^d_{Mn}\left(\boldsymbol{x}; \boldsymbol{Z}^{*(\gamma,\beta)}\right) - Z^{*(\gamma)}_{Mn}(\boldsymbol{x})\right]_{,i} = 0. \tag{8}$$

After invoking the definition of strain and electric field, this relation can be recast in terms of U_M, the mechanical displacement and electric potential, as

$$F_{ijMn} U^d_{M,ni}(\boldsymbol{x}) = F_{ijMn} Z^{*(\gamma)}_{Mn,i}(\boldsymbol{x}). \tag{9}$$

The periodicity of region β implies the periodicity of this perturbed field, as

$$U^d_M(\boldsymbol{x}) = \sum_{\xi} \widetilde{U}^d_M(\xi^\beta) e^{i\xi^\beta\cdot x}, \tag{10}$$

$$\widetilde{U}^d_M(\xi^\beta) = \frac{1}{V}\int_D U^d_M(\boldsymbol{x}) e^{-i\xi^\beta\cdot x} dx. \tag{11}$$

Substitution of (10) and (4) into (9) provides

$$F_{ijMn}\xi^\beta_n\xi^\beta_i \widetilde{U}^d_M(\xi^\beta) = -iF_{ijMn}\xi^\beta_i \widetilde{Z}^{*(\gamma)}_{Mn}(\xi^\beta), \tag{12}$$

which can be solved for $\widetilde{U}^d_M(\xi^\beta)$ as

$$\widetilde{U}^d_M(\xi^\beta) = -iF_{ijKl}\xi^\beta_i \widetilde{Z}^{*(\gamma)}_{Kl}(\xi^\beta) N_{MJ} D^{-1}, \tag{13}$$

where $D(\xi)$ and $N_{MJ}(\xi)$ are, respectively, the determinant and cofactor of $K_{MJ} = F_{iMJn}\xi_n\xi_i$. Mikata (2000) has provided an expression for both $D(\xi)$ and $N_{MJ}(\xi)$ for a transversely isotropic piezoelectric material. Upon substitution of Eq. (13) into (10), one arrives at

$$U^d_M(\boldsymbol{x}) = -i\sum_{\xi^\beta} F_{ijKl}\xi^\beta_i \widetilde{Z}^{*(\gamma)}_{Kl}(\xi^\beta) N_{MJ} D^{-1} e^{i\xi^\beta\cdot x}. \tag{14}$$

The perturbed strain can then be evaluated from Eq. (14), as

$$\begin{aligned} Z^d_{mn}\left(\boldsymbol{x}; \boldsymbol{Z}^{*(\gamma,\beta)}\right) &= \frac{1}{2}\left[U^d_{m,n}(\boldsymbol{x}) + U^d_{n,m}(\boldsymbol{x})\right] \\ &= \frac{1}{2V}\sum_{\xi^{\Omega^\alpha}} F_{ijKl}\left(N_{mJ}\xi^\beta_i\xi^\beta_n + N_{nJ}\xi^\beta_i\xi^\beta_m\right) D^{-1} \\ &\quad \times \int_\beta Z^{*(\gamma)}_{Kl}(\boldsymbol{x}') e^{i\xi^\beta\cdot(x-x')} d\boldsymbol{x}', \quad m = 1, 2, 3. \end{aligned} \tag{15}$$

Likewise for the electric field, we have

$$\begin{aligned} Z^d_{4n}\left(\boldsymbol{x}; \boldsymbol{Z}^{*(\gamma,\beta)}\right) &= U^d_{4,n}(\boldsymbol{x}) \\ &= \frac{1}{V}\sum_{\xi^\beta} F_{ijKl} N_{4J}\xi^\beta_i\xi^\beta_n D^{-1} \int_\beta Z^{*(\gamma)}_{Kl}(\boldsymbol{x}') e^{i\xi^\beta\cdot(x-x')} d\boldsymbol{x}'. \end{aligned} \tag{16}$$

Eqs. (15) and (16) can be combined in an unified expression

$$Z^d_{Mn}\left(\boldsymbol{x}; \boldsymbol{Z}^{*(\gamma,\beta)}\right) = \frac{1}{V}\sum_{\xi^\beta} Q_{MnKl}(\xi^\beta) \int_\beta Z^{*(\gamma)}_{Kl}(\boldsymbol{x}') e^{i\xi^\beta\cdot(x-x')} d\boldsymbol{x}', \tag{17}$$

where

$$Q_{MnKl}(\xi) = \begin{cases} F_{ijKl} D^{-1}\xi_i\left(\xi_n N_{MJ} + \xi_M N_{nJ}\right)/2, & M = 1, 2, 3, \\ F_{ijKl} D^{-1}\xi_i\xi_n N_{MJ}, & M = 4. \end{cases} \tag{18}$$

Now using Eq. (17) and with the aid of the superposition scheme shown in Fig. 3, the overall disturbed strain-electric field at every point throughout the matrix and the equivalent multi-inclusion can be written as

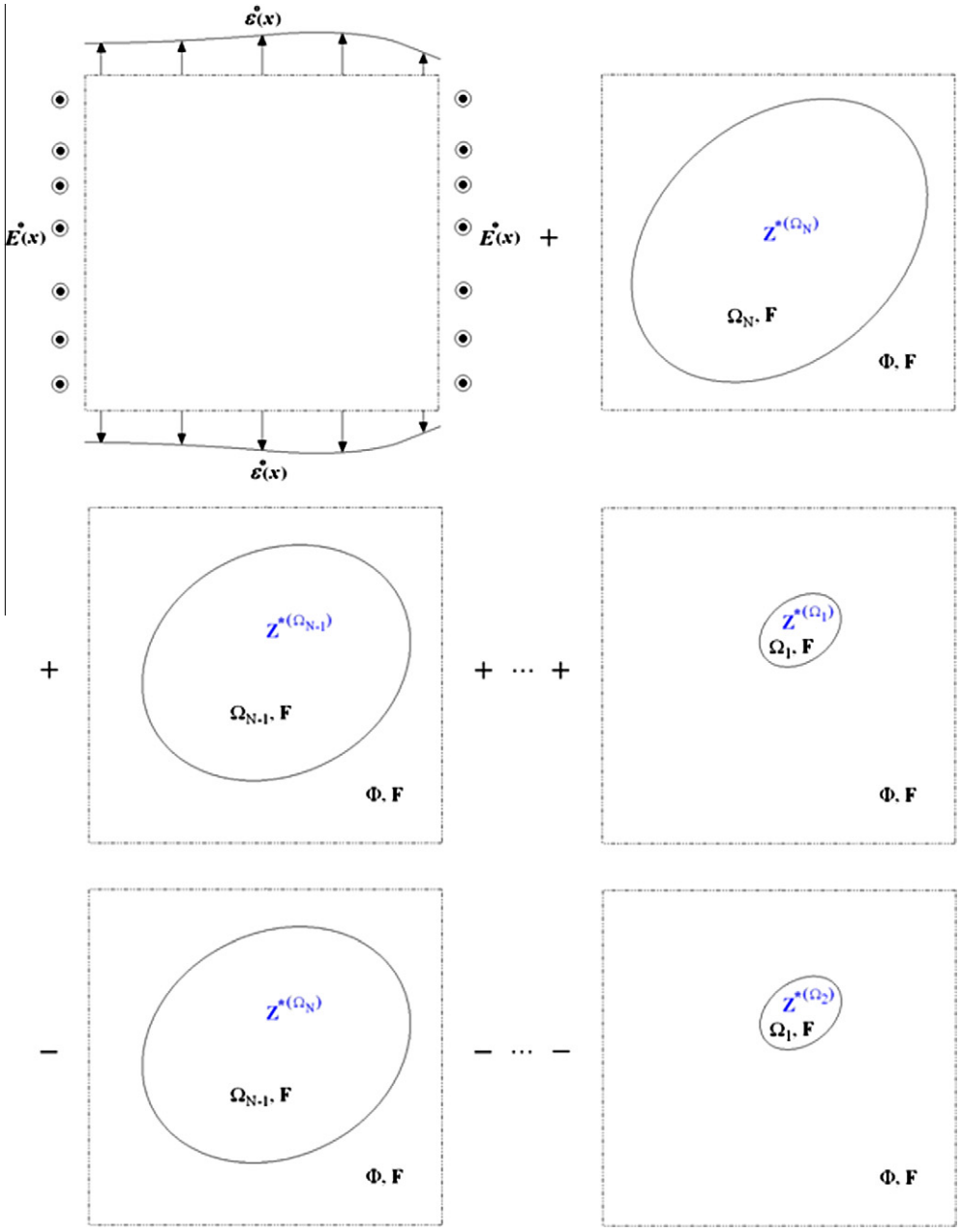

Fig. 3. Decomposition of the equivalent multi-inclusion problem for the determination of the disturbance fields.

$$
\begin{aligned}
Z^d_{Mn}(\boldsymbol{x}) &= \sum_{\alpha=1}^{N} Z^d_{Mn}\left(\boldsymbol{x}; \boldsymbol{Z}^{*(\Omega_\alpha,\psi_\alpha)}\right) - \sum_{\alpha=1}^{N-1} Z^d_{Mn}\left(\boldsymbol{x}; \boldsymbol{Z}^{*(\Omega_{\alpha+1},\psi_\alpha)}\right) \\
&= \sum_{\alpha=1}^{N-1}\left[Z^d_{Mn}\left(\boldsymbol{x}; \boldsymbol{Z}^{*(\Omega_\alpha,\psi_\alpha)}\right) - Z^d_{Mn}\left(\boldsymbol{x}; \boldsymbol{Z}^{*(\Omega_{\alpha+1},\psi_\alpha)}\right)\right] \\
&\quad + Z^d_{Mn}\left(\boldsymbol{x}; \boldsymbol{Z}^{*(\Omega_N,\psi_N)}\right) \\
&= \frac{1}{V}\sum_{\alpha=1}^{N-1}\sum_{\xi^{\psi_\alpha}} Q_{MnKl}\left(\xi^{\psi_\alpha}\right)\int_{\psi_\alpha}\left[Z^{*(\Omega_\alpha)}_{Kl}(\boldsymbol{x}') - Z^{*(\Omega_{\alpha+1})}_{Kl}(\boldsymbol{x}')\right]e^{i\xi^{\psi_\alpha}\cdot(x-x')}d\boldsymbol{x}' \\
&\quad + \frac{1}{V}\sum_{\xi^{\psi_N}} Q_{MnKl}\left(\xi^{\psi_N}\right)\int_{\psi_N} Z^{*(\Omega_N)}_{Kl}(\boldsymbol{x}')e^{i\xi^{\psi_N}\cdot(x-x')}d\boldsymbol{x}'. \qquad (19)
\end{aligned}
$$

To obtain the equivalent eigenstrain-electric field pertinent to the αth phase, we now recall Eshelby's equivalent inclusion principle in the local form

$$
\begin{aligned}
\Sigma^o_{ij} + \Sigma^d_{ij}(x) &= F^{\Omega_\alpha}_{ijMn}\left(Z^o_{Mn} + Z^d_{Mn}(\boldsymbol{x})\right) \\
&= F_{ijMn}\left(Z^o_{Mn} + Z^d_{Mn}(\boldsymbol{x}) - Z^{*(\Omega_\alpha)}_{Mn}(\boldsymbol{x})\right), \quad \boldsymbol{x}\in\Omega_\alpha,\ \alpha = 1,2,\ldots,N. \qquad (20)
\end{aligned}
$$

Since only the average field is needed for the calculation of effective moduli, this local form can be integrated over each subdomain to yield the averaged quantities

$$
\begin{aligned}
\left\langle \Sigma^o_{ij}\right\rangle_{\Omega_\alpha} + \left\langle \Sigma^d_{ij}(\boldsymbol{x})\right\rangle_{\Omega_\alpha} &= F^{\Omega_\alpha}_{ijMn}\left(Z^o_{Mn} + \left\langle Z^d_{Mn}(\boldsymbol{x})\right\rangle_{\Omega_\alpha}\right) \\
&= F_{ijMn}\left(Z^o_{Mn} + \left\langle Z^d_{Mn}(x)\right\rangle_{\Omega_\alpha} - \left\langle Z^{*(\Omega_\alpha)}_{Mn}(\boldsymbol{x})\right\rangle_{\Omega_\alpha}\right), \\
&\quad \boldsymbol{x}\in\Omega_\alpha,\ \alpha = 1,2,\ldots,N, \qquad (21)
\end{aligned}
$$

where the brackets $\langle\bullet\rangle_{\Omega_\alpha}$ denote the volume average of the said quantity. The volume average of $Z^d_{Mn}(x)$ over the αth phase in turn can be evaluated from Eq. (19), as

$$\left\langle Z^{d}_{Mn}(\boldsymbol{x})\right\rangle_{\Omega_\alpha} = \frac{1}{VV^{\Omega_\alpha}}\sum_{\omega=1}^{N-1}\sum_{\xi^{\psi_\omega}} Q_{MnKl}(\xi)H_{\Omega_\alpha}(\xi) \times \int_{\psi_\omega}\left[Z^{*(\Omega_\omega)}_{Kl}(\boldsymbol{x}') - Z^{*(\Omega_{\omega+1})}_{Kl}(\boldsymbol{x}')\right]e^{-i\xi^{\psi_\omega}\cdot x'}d\boldsymbol{x}' + \frac{1}{VV^{\Omega_\alpha}}\sum_{\xi^{\psi_N}} Q_{MnKl}(\xi)H_{\Omega_\alpha}(\xi) \times \int_{\psi_N} Z^{*(\Omega_N)}_{Kl}(\boldsymbol{x}')e^{-i\xi^{\psi_N}\cdot x'}d\boldsymbol{x}', \tag{22}$$

in which $H_{\Omega_\alpha}(\xi) = \int_{\Omega_\alpha} e^{i\xi\cdot x}d\boldsymbol{x}$ is readily available with the aid of

$$\int_{\psi_\alpha} e^{i\xi\cdot x}d\boldsymbol{x} = \frac{3(\sin\eta - \eta\cos\eta)}{\eta^3}V^{\psi_\alpha},$$
$$\eta = \sqrt{(a_1\xi_1)^2 + (a_2\xi_2)^2 + (a_3\xi_3)^2}, \tag{23}$$

where a_i, $i = 1, 2, 3$ are the principle half-axes of the ellipsoidal domain. Finally, substituting Eq. (22) into the second equality of Eq. (21), and after some rearrangement, we obtain

$$Z^{o}_{Mn} = \left[F_{ijMn} - F^{\Omega_\alpha}_{ijMn}\right]^{-1}F_{ijKl}\left\langle Z^{*(\Omega_\alpha)}_{Kl}\right\rangle_{\Omega_\alpha} - \frac{1}{VV^{\Omega_\alpha}}\sum_{\omega=1}^{N-1}\sum_{\xi^{\psi_\omega}} Q_{MnKl}(\xi)H_{\Omega_\alpha}(\xi) \times \int_{\psi_\omega}\left[Z^{*(\Omega_\omega)}_{Kl}(\boldsymbol{x}') - Z^{*(\Omega_{\omega+1})}_{Kl}(\boldsymbol{x}')\right]e^{-i\xi^{\psi_\omega}\cdot x'}d\boldsymbol{x}' - \frac{1}{VV^{\Omega_\alpha}}\sum_{\xi^{\psi_N}} Q_{MnKl}(\xi)H_{\Omega_\alpha}(\xi)\int_{\psi_N} Z^{*(\Omega_N)}_{Kl}(\boldsymbol{x}')e^{-i\xi^{\psi_N}\cdot x'}d\boldsymbol{x}', \quad \boldsymbol{x}\in\Omega_\alpha,\ \alpha = 1,2,\ldots,N. \tag{24}$$

When this relation is written for all N subdomains, it provides N simultaneous equations for $\left\langle Z^{*(\Omega_\alpha)}_{Mn}\right\rangle_{\Omega_\alpha}$, which then can be solved in terms of the prescribed Z^{o}_{Mn}. The complex structure of Eq. (24) suggests a method for estimating $\left\langle Z^{*(\Omega_\alpha)}_{Mn}\right\rangle_{\Omega_\alpha}$ in terms of the prescribed Z^{o}_{Mn}, in which the eigenfield in each phase will be replaced by its average value, leading to

$$Z^{o}_{Mn} = \left[F_{ijMn} - F^{\Omega_\alpha}_{ijMn}\right]^{-1}F_{ijKl}\left\langle Z^{*(\Omega_\alpha)}_{Kl}\right\rangle_{\Omega_\alpha} - \frac{1}{VV^{\Omega_\alpha}}\sum_{\omega=1}^{N-1}\sum_{\xi^{\psi_\omega}} Q_{MnKl}(\xi)H_{\Omega_\alpha}(\xi)H_{\psi_\omega}(-\xi) \times \left[\left\langle Z^{*(\Omega_\omega)}_{Kl}\right\rangle_{\Omega_\omega} - \left\langle Z^{*(\Omega_{\omega+1})}_{Kl}\right\rangle_{\Omega_{\omega+1}}\right] - \frac{1}{VV^{\Omega_\alpha}}\sum_{\xi^{\psi_N}} Q_{MnKl}(\xi)H_{\Omega_\alpha}(\xi)H_{\psi_N}(-\xi)\left\langle Z^{*(\Omega_N)}_{Kl}\right\rangle_{\Omega_N}, \quad \boldsymbol{x}\in\Omega_\alpha,\ \alpha = 1,2,\ldots,N, \tag{25}$$

where $H_{\psi_\omega}(-\xi) = \int_{\psi_\omega} e^{-i\xi\cdot x'}d\boldsymbol{x}'$. We thus have N equations for the N unknowns, $\left\langle Z^{*(\Omega_\alpha)}_{Mn}\right\rangle_{\Omega_\alpha}$. The result can be expressed in the general form

$$\left\langle Z^{*(\Omega_\alpha)}_{Mn}\right\rangle_{\Omega_\alpha} = A^{*(\Omega_\alpha)}_{MnKl}Z^{o}_{Kl}, \tag{26}$$

where $\boldsymbol{A}^*$ is the eigenfield concentration tensor of the said domain.

This formulation has several desirable features built into it. For instance the quantity $H(\xi)$ can reflect the geometry of the particle core and its coatings, and the infinite series can account for the particle–particle interactions. Moreover, since the core and the coating layers can have distinct periodicity in present formulation, this method is quite versatile, and it can be applied to a wide range of coating problems, thin or thick, single or multi-layers, and even eccentric coating.

4. Effective electroelastic moduli tensor, $\overline{F}_{ijMn}$

We now seek to estimate the overall electromechanical moduli of the periodic piezoelectric composite by considering the energy equivalence between the heterogeneous medium and the effective homogeneous medium. Under an uniform far-field, Z^{o}_{Mn}, and denoting the effective moduli tensor by $\overline{F}_{ijMn}$, the total energy (the electric Gibbs energy) of the effective medium can be written as

$$U = \frac{V}{2}\overline{F}_{ijMn}Z^{o}_{Ji}Z^{o}_{Mn}. \tag{27}$$

On the other hand for the equivalent multi-inclusion system, it is given by

$$U = \frac{V}{2}F_{ijMn}Z^{o}_{Ji}Z^{o}_{Mn} - \frac{1}{2}F_{ijMn}Z^{o}_{Mn}\sum_{\alpha=1}^{N}V^{\Omega_\alpha}\left\langle Z^{*(\Omega_\alpha)}_{Ji}(\boldsymbol{x})\right\rangle_{\Omega_\alpha}, \tag{28}$$

where the volume of the phase, V^{Ω_α}, provides the weighted mean for each average equivalent eigenfield in the summation. The effective electromechanical moduli of the periodic piezoelectric composite then can be calculated from

$$\overline{F}_{ijMn}Z^{o}_{Ji}Z^{o}_{Mn} = F_{ijMn}Z^{o}_{Ji}Z^{o}_{Mn} - F_{ijMn}Z^{o}_{Mn}\sum_{\alpha=1}^{N}f^{\Omega_\alpha}\left\langle Z^{*(\Omega_\alpha)}_{Ji}\right\rangle_{\Omega_\alpha}, \tag{29}$$

where f^{Ω_α} is the associated volume fraction of each layer Ω_α, $\alpha = 1,2,\ldots,N$. Recalling Eq. (26) and noting the symmetry, $F_{lKMn} = F_{nMKl}$, the effective electroelastic moduli tensor of the multi-coated composite with periodic microstructure can be expressed as

$$\overline{F}_{ijMn} = F_{ijMn} - F_{ijKl}\left(\sum_{\alpha=1}^{N}f^{\Omega_\alpha}A^{*(\Omega_\alpha)}_{KlMn}\right) \quad \text{or}$$
$$\overline{F} = F\left[I - \left(\sum_{\alpha=1}^{N}f^{\Omega_\alpha}A^{*(\Omega_\alpha)}\right)\right], \tag{30}$$

in the matrix form, where I is the fourth-order identity tensor.

5. Results and discussion

To place the generality and the robustness of the developed methodology in perspective, we now apply it to several problems of various complexities. The effect of some microstructure parameters, such as thickness, eccentricity, and shape, as well as the effect of electroelastic properties of the periodic particle and their coatings on the overall properties of the composite, will be demonstrated.

Before we proceed, it is noteworthy to mention that, when dealing with high concentration of particles or high property contrast among the phases, the variation of eigenfield within the phase can be highly non-uniform. We have found that, by dividing a thick layer into several thin layers, the computed results are more accurate. This is not to say that the field in a thin layer is homogeneous as it is not (see Cherkaoui et al., 1995), but we have replaced this thin layer effect through its mean from Eq. (20) to Eq. (21), and this additional subdivision would allow us to account for the field heterogeneity along the radial direction more precisely. In addition, we have also observed that the summation over the infinite series also always converges. This can be seen from the fact that function $Q_{MnKl}(\xi)$ remains finite as ξ_i, $i = 1, 2, 3$ takes on large values, and that the integral terms $H_{\Omega_\alpha}(\xi)$ and $H_{\psi_\omega}(-\xi)$ in the series go to zero like $1/\xi_i^2$ as ξ_i approaches to infinity. Accordingly, the infinite series in Eq. (25) are of order $1/\xi_i^4$ for large value of ξ_i, and this leads to rapid convergence.

To verify the accuracy of present approach, we will first make comparisons with existing results of single-phase inhomogeneities and of thinly-coated inhomogeneities in Sections 5.1 and 5.2, and

Table 1
Electroelastic properties of piezocomposite constituents, C_{ijkl} (GPa), e_{ijk} (C/m^2), $K_o = 8.85 \times 10^{-12}$ (C/Vm).

	C_{1111}	C_{1122}	C_{1133}	C_{3333}	C_{1313}	e_{311}	e_{333}	e_{113}	K_{11}/K_o	K_{33}/K_o
PZT-7A	148	76.2	74.2	131	25.4	−2.1	9.5	9.2	460	235
Epoxy	8	4.4	4.4	8	1.8	0	0	0	4.2	4.2
Glass	88.8	29.6	29.6	88.8	29.6	0	0	0	6.4	6.4
VDF/TeFE	4.63	2.95	2.95	4.63	0.834	0	−0.177	0	10.7	10.7

with the result of average electric field in the fiber within a three-phase elliptic inclusion system in Section 5.3. In Section 5.4, we will study the effective electroelastic properties of a piezocomposite with thickly coated reinforcements. In this case the applicability of the present theory to functionally graded coating will also be demonstrated. In Section 5.5, we will study the behavior of a piezoelectric composite having periodic voids with elastic coating, and finally in Section 5.6, we will explore the effect of thick coating layers with variable thickness on the overall properties of the composite.

It should be mentioned that in computations a simple center-cubic distribution of reinforcements is assumed in Sections 5.1 and 5.2, while a simple cubic configuration is assumed for Sections 5.3–5.6. In all cases the piezoelectric phase is taken to be transversely isotropic, with the poling direction pointing along direction x_3. Except for the last problem, the Cartesian coordinates are chosen to coincide with the principle axes of the ellipsoidal domain of inhomogeneities. The material properties used in the calculations are listed in Table 1, but the Poisson's ratio of each isotropic constituent is assumed to be equal to 1/3 if not listed there. In Sections 5.4–5.6, the obtained results are presented in the normalized form

$$\widetilde{F}_{iJMn} = \overline{F}_{iJMn} \Big/ F^{PZT-7A}_{iJMn}, \tag{31}$$

with respect to those of PZT-7A (no summation over the indices).

5.1. Comparison with Wei et al. (2006) for periodic PZT-7A spherical particles in a polymer matrix

We first consider a piezoelectric composite consisting of single-phase PZT-7A spherical particles distributed periodically within a polymeric VDF/TrFE matrix. Such a problem has been examined by Wei et al. (2006), so this study will serve to make contact with the existing literature. The present micromechanical approach is applied to this problem by subdividing the single-phase PZT inhomogeneity into one particle core and five coating layers with the same material properties. Fig. 4 displays the effective piezoelectric coefficient, $\bar{d}_{333} = \bar{e}_{3ij}\overline{C}^{-1}_{ij33}$ (usually call d_{33} in the literature) as a function of volume fraction of reinforcements. It is observed that the result of the proposed methodology is in excellent agreement with the one reported by Wei et al. (2006). Both indicate that this effective piezoelectric constant increases steadily with the inhomogeneity concentration.

5.2. Comparison with Dinzart and Sabar (2009) and Hori and Nemat-Nasser (1993, 1994) for randomly distributed long glassy fibers with thin PZT-7A coating in an epoxy matrix

To illustrate the effect of a piezoelectric coating layer, the piezocomposite is taken to consist of periodic glassy fibers coated by a thin PZT-7A piezoelectric layer embedded in an epoxy matrix. Let a_p, $p = 1, 2, 3$, be the principle half-axes of the inhomogeneity core, with $a_2/a_1 = 1$ and $a_3/a_1 = 100$. A similar problem was most recently studied by Dinzart and Sabar (2009), except that the coated particles were randomly distributed, so the comparison must be viewed in this light. Their formulation made use of Mori–Tanaka's (1973) method and Hill's (1983) interfacial operator, with a specific objective of investigating the condition of a thin layer of coating. We have employed the present method to calculate the effective piezoelectric coefficient, $\bar{d}_{333}$, for several thickness ratios of the coating layer, $\Delta a_1/a_1 = 0.02$, 0.05 and 0.1, as a function of the volume fraction of glassy cores. To make further comparison we have also employed the double-inclusion model (Hori and Nemat-Nasser, 1993, 1994; Li, 2000) for random piezocomposites to treat this

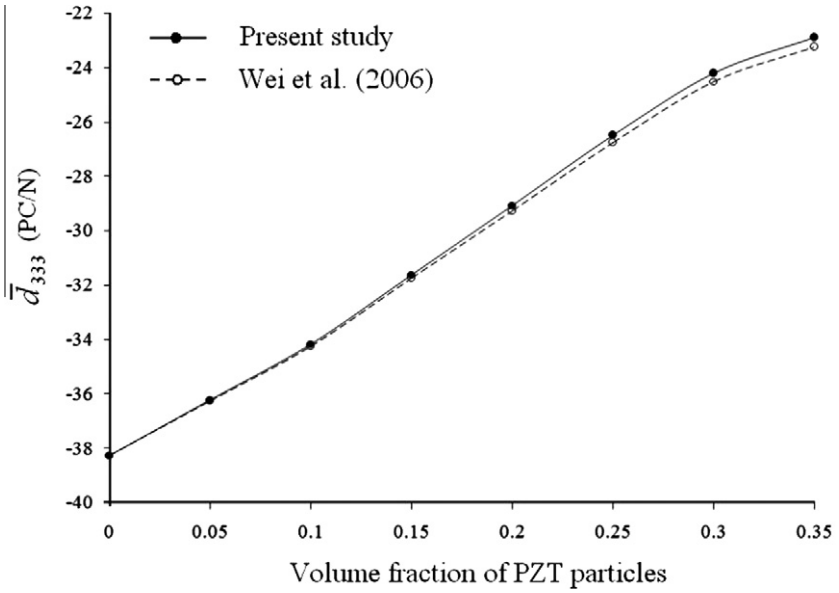

Fig. 4. The effective piezoelectric coefficient of the piezocomposite with single-phase spherical inhomogeneities (PZT-VDF/TrFE).

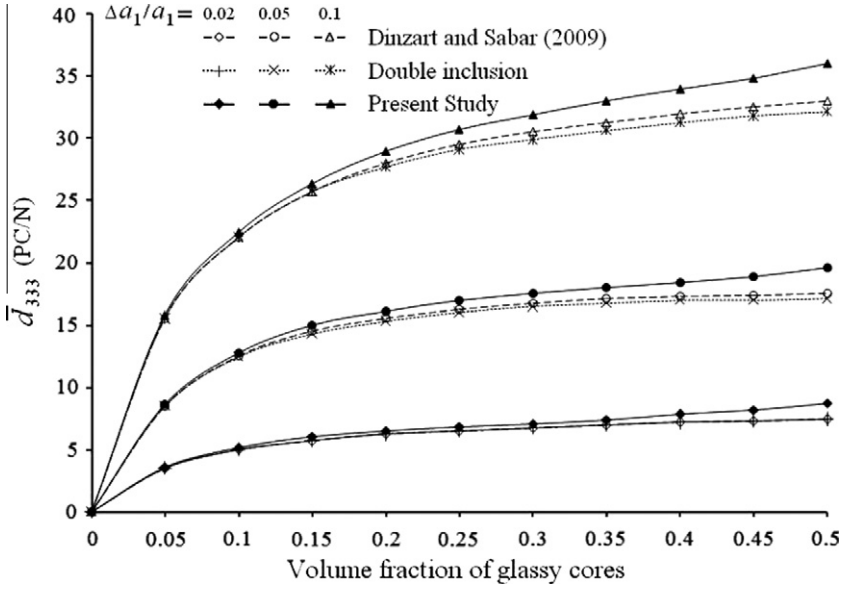

Fig. 5. Effective piezoelectric constants of a piezocomposite based on the periodic glass particles with thin PZT-7A coating, and comparison with Dinzart and Sabar (2009), and the double-inclusion model of Hori and Nemat-Nasser (1993, 1994) for a similar piezocomposite but without periodic structure.

problem. Our results with periodic structure and those of Dinzart and Sabar (2009) and double-inclusion model are illustrated in Fig. 5. It is readily observed that for the dilute concentration of particles, the latter three sets of results are very close to each other, but the results with periodic distribution of the inhomogeneities are slightly higher than these two; such a difference is somewhat expected. But all results indicate that, by increasing the thickness ratio from 2% to 10%, this piezoelectric constant can increase by 300% at the fiber concentration of 0.5. It strongly points to the significance of a piezoelectric coating layer.

5.3. Comparison with Sudak (2003) for the average electroelastic field in periodically distributed elliptically coated cylinders under in-plane electric field

To verify the validity of the developed method further, let us consider the case of a piezocomposite system containing elliptic coated cylinders. Here the fiber-coating and coating-matrix interfaces are represented by two elliptic layers of the same foci, and their principle axes, (a_1,a_2) and (a_1',a_2'), also coincide. The issue to be examined is the influence of thickness and material properties of the interphase layer on the induced average electric field within the core fiber under remote in-plane electric field, $\left(\sigma_{ij}^o = 0,\ E_i^0 = E_2^0\right)$. Sudak (2003) has solved a related problem involving a single coated fiber in an infinite matrix. By means of the potential functions and complex variables, he provided the exact solution for the electroelastic field as a function of relative thickness of interphase layer, where ρ_1 and ρ_2 are the radii of concentric circles obtained from the conformal mapping of the elliptic cross sections. In order to make comparison with Sudak's results, we have adopted the same electroelastic moduli for the core fiber: $C_{1313}^f = 35.3$ GPa, $e_{113}^f = 10\ \mathrm{C/m^2}$ and $K_{11}^f = 15.1\ \mathrm{nC^2/Nm^2}$. In addition the material properties of the coating and matrix are given by C_{1313}^c/C_{1313}^f=0.1, C_{1313}^m/C_{1313}^f=0.5, K_{11}^c/K_{11}^f=0.2, K_{11}^m/K_{11}^f=3 and $e_{113}^m/e_{113}^f = 0.6$. The influence of aspect ratio and piezoelectric constant of coating has been studied for the two different cases: (1) $e_{113}^c/e_{113}^f = -3,\ \rho_1^2 = 2$, and (2) $e_{113}^c/e_{113}^f = 3,\ \rho_1^2 = 4$.

To make contact with Sudak's results of a single coated inhomogeneity in an infinite matrix, the volume fractions of core fiber and its coating are kept fixed at the very low concentration, $f^f + f^c = 5\%$. Moreover, in the present analysis, the influence of sub-layers thickness on the accuracy of our results is also examined by subdividing the pertinent coating layer into four different numbers of sub-layers: N^c = 1, 6, 12 and 18, which are all confocal. The normalized electric fields in the core fiber estimated by the present theory together with the results of Sudak (2003) are depicted in Fig. 6 as a function of relative thickness of coating, α. It is readily observed that, as the number of sub-layers increases from 1 to 18, the average electric field in the elliptic fiber also increases steadily, but the results between N^c = 12 and 18 are very close, indicating that the results have reached the convergent state. Comparison of the results at the convergent state with Sudak's exact solution is generally satisfactory for the two cases considered, notwithstanding a larger discrepancy at smaller α. This comparison indicates that, for accuracy, it is necessary to increase the number of sub-layers to the point that the computed results have reached the fully convergent state.

5.4. Periodic spherical PZT-7A particles coated by thick or functionally graded piezoelectric layer

Suppose that the concentric coated PZT-7A spherical particles are distributed periodically in a non-piezoelectric isotropic matrix. Here we study two types of coating on the PZT particles:

(i) A non-piezoelectric isotropic coating with stiffness ratios of $C_{1313}^{coating}/C_{1313}^{matrix} = 0.1$ and 2, and dielectric constant ratio of $K_{ij}^{coating}/K_0 = 5$, and
(ii) A functionally graded piezoelectric (FGP) coating with its electroelastic properties vary linearly from those of the core to the matrix, as

$$C_{ijkl}^{coating} = C_{ijkl}^{core} + \left(C_{ijkl}^{matrix} - C_{ijkl}^{core}\right)\left(\frac{r - r^{core}}{t}\right),$$
$$K_{ij}^{coating} = K_{ij}^{core} + \left(K_{ij}^{matrix} - K_{ij}^{core}\right)\left(\frac{r - r^{core}}{t}\right),$$
$$e_{ijk}^{coating} = e_{ijk}^{core} + \left(e_{ijk}^{matrix} - e_{ijk}^{core}\right)\left(\frac{r - r^{core}}{t}\right), \tag{32}$$

where t is the thickness of coating layer, r is radial distance form center of core and r^{core} is the radius of the PZT-7A inhomogeneity

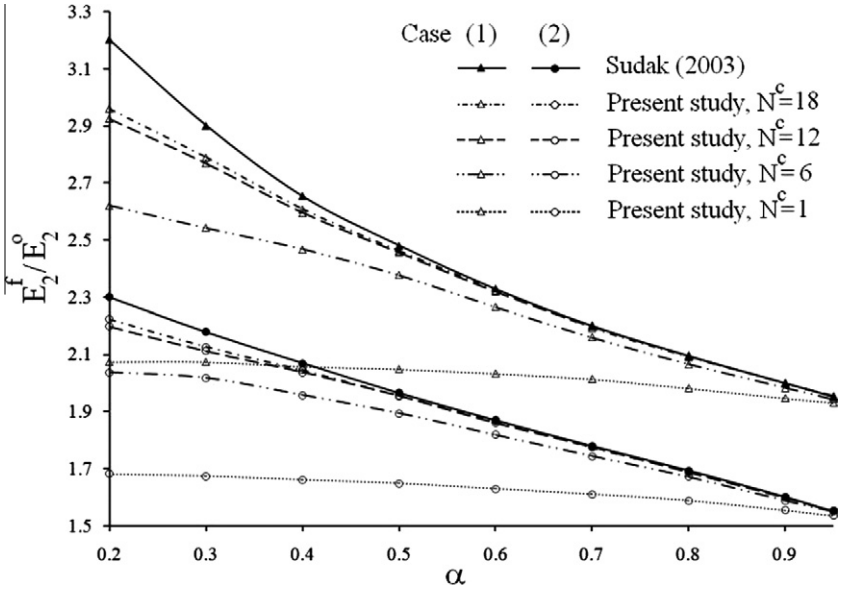

Fig. 6. Comparison with Sudak (2003) for the dependence of average electroelastic field in an elliptic coated cylinder on α under in-plane electric field. Here $\alpha = (\rho_1/\rho_2)^2$, $f^f + f^c = 0.05$, and case (1) $e^c_{113}/e^f_{113} = -3$, $\rho_1^2 = 2$, and case (2) $e^c_{113}/e^f_{113} = 3$, $\rho_1^2 = 4$.

core. In both cases we have examined the effect of rigidity of the host matrix with respect to the rigidity of the core through varying the ratio $C^{matrix}_{1313}/C^{core}_{1313} = 0.5$ and 2, representing the cases that matrix is, respectively, softer and stiffer than the PZT-7A core.

We have applied the developed theory to calculate these effective moduli for the stated problems. The results for the volume fractions of f^{core} = 15% and 30% are given in Tables 2 and 3, respectively. In each table the elastic properties are listed in (a), and the piezoelectric and dielectric constants listed in (b), for clarity. Note that the overall material possesses the tetragonal symmetry and consequently there are six elastic, three piezoelectric and two dielectric constants.

A closer look at the listed data shows the following characteristics:

(i) From Table 2a, it is observed that, when the matrix is elastically stiffer than the core $\left(C^{matrix}_{1313}/C^{core}_{1313} = 2\right)$, the enhancement of the overall stiffness further depends on whether the coating is stiffer than then matrix. If it does, then the overall stiffness will also increase with increasing coating concentration. Otherwise, it decreases with it. When the coating is a functionally graded piezoelectric phase, the overall stiffness tends to decrease with increasing coating concentration.

(ii) When the matrix is elastically softer than the core $\left(C^{matrix}_{1313}/C^{core}_{1313} = 0.5\right)$, the same trends holdwith the non-piezoelectric inclusions, but with the FGPM coating the overall stiffness tends to increase.

(iii) From Table 2b, the same trend is observed for the piezoelectric constants, but a reversed trend is found for the dielectric constants. With the functionally graded piezoelectric coating, both the piezoelectric and dielectric constants tend to increase with increasing coating concentration, regardless of the condition whether the matrix is elastically stiffer or softer than the core.

(iv) At the higher core concentration of $f^{core} = 0.30$, the results are shown in Tables 3a and 3b. It is seen that, with the non-piezoelectric coating, the trend for the elastic stiffness remains the same, but that with the FGP coating it is now reversed. The trends for the piezoelectric and dielectric constants remain the same as with the case of $f^{core} = 0.15$.

The foregoing characteristics reflect the complex nature of interplay between the properties of core, matrix, and coating, as well as whether the coating is an uniform material or a function-

Table 2a
Effective elastic properties of piezocomposites containing coated spherical particles for volume fraction of inhomogeneity core, f^{core} = 0.15.

$\frac{C^{matrix}_{1313}}{C^{core}_{1313}}$	$\frac{C^{coating}_{1313}}{C^{matrix}_{1313}}$	$f^{coating}$	$\tilde{C}_{1111}$	$\tilde{C}_{1212}$	$\tilde{C}_{1122}$	$\tilde{C}_{3333}$	$\tilde{C}_{1313}$	$\tilde{C}_{1133}$
2	No coating	0	1.374	1.483	1.173	1.423	2.31	1.195
	0.1	0.03	1.322	1.425	1.095	1.361	2.266	1.127
		0.09	1.294	1.398	0.974	1.298	2.191	1.009
	2	0.03	1.397	1.505	1.149	1.472	2.290	1.228
		0.09	1.428	1.549	1.215	1.522	2.406	1.249
	FGP	0.03	1.353	1.465	1.125	1.39	2.285	1.164
		0.09	1.329	1.45	0.992	1.357	2.244	1.14
0.5	No coating	0	0.356	0.412	0.294	0.385	0.560	0.301
	0.1	0.03	0.329	0.400	0.280	0.366	0.547	0.29
		0.09	0.318	0.377	0.265	0.351	0.532	0.276
	2	0.03	0.365	0.428	0.315	0.409	0.577	0.325
		0.09	0.385	0.449	0.331	0.417	0.592	0.246
	FGP	0.03	0.359	0.422	0.308	0.397	0.571	0.313
		0.09	0.364	0.435	0.319	0.408	0.783	0.330

Table 2b
Effective piezoelectric and dielectric properties of piezocomposites containing coated spherical particles for volume fraction of inhomogeneity core, $f^{core} = 0.15$.

$\frac{C_{1313}^{matrix}}{C_{1313}^{core}}$	$\frac{C_{1313}^{coating}}{C_{1313}^{matrix}}$	$f^{coating}$	$\tilde{e}_{311}$	$\tilde{e}_{333}$	$\tilde{e}_{113}$	$\tilde{K}_{11}$	$\tilde{K}_{33}$
2	No coating	0	0.112	0.135	0.108	0.172	0.189
	0.1	0.03	0.109	0.131	0.098	0.181	0.195
		0.09	0.095	0.127	0.091	0.189	0.207
	2	0.03	0.119	0.141	0.116	0.165	0.18
		0.09	0.13	0.156	0.128	0.159	0.173
	FGP	0.03	0.179	0.193	0.172	0.198	0.219
		0.09	0.205	0.23	0.198	0.215	0.228
0.5	No coating	0	0.117	0.142	0.115	0.157	0.17
	0.1	0.03	0.109	0.135	0.108	0.163	0.179
		0.09	0.1	0.127	0.096	0.171	0.188
	2	0.03	0.121	0.148	0.121	0.151	0.161
		0.09	0.128	0.155	0.125	0.143	0.153
	FGP	0.03	0.195	0.21	0.187	0.166	0.181
		0.09	0.225	0.286	0.216	0.184	0.196

Table 3a
Effective elastic properties of piezocomposites containing coated spherical particles for volume fraction of inhomogeneity core, $f^{core} = 0.30$.

$\frac{C_{1313}^{matrix}}{C_{1313}^{core}}$	$\frac{C_{1313}^{coating}}{C_{1313}^{matrix}}$	$f^{coating}$	$\tilde{C}_{1111}$	$\tilde{C}_{1212}$	$\tilde{C}_{1122}$	$\tilde{C}_{3333}$	$\tilde{C}_{1313}$	$\tilde{C}_{1133}$
2	No coating	0	1.221	1.302	1.109	1.215	2.019	1.147
	0.1	0.06	1.153	1.275	1.072	1.149	1.902	1.11
		0.18	0.109	1.22	0.892	1.077	1.657	0.98
	2	0.06	1.413	1.347	1.2	1.571	2.395	1.24
		0.18	1.472	1.389	1.227	1.607	2.471	1.265
	FGP	0.06	1.184	1.319	1.093	1.182	1.932	1.133
		0.18	1.57	1.271	0.965	1.119	1.803	1.106
0.5	No coating	0	0.388	0.43	0.316	0.408	0.583	0.325
	0.1	0.06	0.34	0.417	0.302	0.396	0.562	0.311
		0.18	0.328	0.389	0.289	0.38	0.549	0.297
	2	0.06	0.402	0.457	0.342	0.427	0.605	0.338
		0.18	0.418	0.492	0.358	0.44	0.623	0.365
	FGP	0.06	0.396	0.446	0.329	0.418	0.597	0.332
		0.18	0.409	0.459	0.348	0.429	0.613	0.35

ally graded material. Functionally graded piezoelectric materials (FGPMs) represent an emerging class of smart materials that allow the properties to be tailored through judicious choice of property gradient. Their applications can have significant benefit to both static and dynamic fracture strength (Li and Weng, 2002a,b), and to the fatigue strength (Zhu et al., 2000) of a material. For the precise nature of the overall electromechanical properties, a full execution of computation is required.

5.5. Periodic spheroidal voids coated with thick non-piezoelectric layer in a PZT-7A matrix

Consider a PZT-7A piezoelectric material containing coated spheroidal voids, with $a_2 = a_1 \leqslant a_3$, where their slenderness is determined by variation of the aspect ratio, a_3/a_1. Let the coating layer be an isotropic material with rigidity ratios of $C_{1313}^{coating}/C_{1313}^{matrix} = 0.5$ and 2.5, and dielectric constant ratios of $K_{ij}^{coating}/K_0 = 5$, where K_0 is

Table 3b
Effective piezoelectric and dielectric properties of piezocomposites containing coated spherical particles for volume fraction of inhomogeneity core, $f^{core} = 0.30$.

$\frac{C_{1313}^{matrix}}{C_{1313}^{core}}$	$\frac{C_{1313}^{coating}}{C_{1313}^{matrix}}$	$f^{coating}$	$\tilde{e}_{311}$	$\tilde{e}_{333}$	$\tilde{e}_{113}$	$\tilde{K}_{11}$	$\tilde{K}_{33}$
2	No coating	0	0.21	0.283	0.197	0.322	0.35
	0.1	0.06	0.198	0.268	0.171	0.338	0.366
		0.18	0.187	0.25	0.159	0.34	0.379
	2	0.06	0.226	0.301	0.208	0.314	0.335
		0.18	0.233	0.319	0.215	0.306	0.322
	FGP	0.06	0.305	0.356	0.28	0.333	0.369
		0.18	0.337	0.392	0.309	0.351	0.381
0.5	No coating	0	0.252	0.311	0.217	0.295	0.321
	0.1	0.06	0.238	0.29	0.199	0.329	0.357
		0.18	0.22	0.269	0.178	0.337	0.365
	2	0.06	0.268	0.321	0.222	0.272	0.309
		0.18	0.29	0.35	0.251	0.26	0.289
	FGP	0.06	0.351	0.402	0.297	0.325	0.357
		0.18	0.39	0.436	0.315	0.346	0.376

Table 4a
Effective elastic properties of porous piezoelectric materials containing coated spherical voids, with $a_3/a_1 = 1$.

f^{void}	$f^{coating}$	$\frac{C^{coating}_{1313}}{C^{matrix}_{1313}}$	$\widetilde{C}_{1111}$	$\widetilde{C}_{1212}$	$\widetilde{C}_{1122}$	$\widetilde{C}_{3333}$	$\widetilde{C}_{1313}$	$\widetilde{C}_{1133}$
0.2	0	No coating	0.731	0.671	0.69	0.744	0.652	0.675
	0.04	0.5	0.709	0.649	0.661	0.715	0.638	0.65
		2.5	0.752	0.693	0.72	0.761	0.681	0.711
	0.08	0.5	0.675	0.618	0.62	0.681	0.604	0.611
		2.5	0.798	0.715	0.764	0.805	0.733	0.758
0.3	0	No coating	0.569	0.532	0.531	0.586	0.503	0.512
	0.06	0.5	0.54	0.505	0.505	0.552	0.49	0.487
		2.5	0.601	0.55	0.559	0.617	0.531	0.544
	0.12	0.5	0.508	0.482	0.469	0.518	0.471	0.456
		2.5	0.65	0.582	0.593	0.662	0.579	0.585

Table 4b
Effective piezoelectric and dielectric properties of porous piezoelectric materials containing coated spherical voids, with $a_3/a_1 = 1$.

f^{void}	$f^{coating}$	$\frac{C^{coating}_{1313}}{C^{matrix}_{1313}}$	$\tilde{e}_{311}$	$\tilde{e}_{333}$	$\tilde{e}_{113}$	$\widetilde{K}_{11}$	$\widetilde{K}_{33}$
0.2	0	No coating	0.436	0.691	0.643	0.775	0.803
	0.04	0.5	0.416	0.669	0.617	0.74	0.762
		2.5	0.422	0.674	0.627	0.748	0.766
	0.08	0.5	0.405	0.642	0.591	0.697	0.727
		2.5	0.414	0.65	0.611	0.703	0.738
0.3	0	No coating	0.187	0.514	0.501	0.663	0.735
	0.06	0.5	0.169	0.496	0.478	0.61	0.684
		2.5	0.177	0.507	0.485	0.633	0.702
	0.12	0.5	0.151	0.469	0.441	0.517	0.613
		2.5	0.16	0.483	0.462	0.551	0.601

the dielectric permittivity of vacuum. Assuming $a_3/a_1 = 1$ and 10, the effective electroelastic moduli of the resultant material for selected values of f^{void} and $f^{coating}$, and as a function of $C^{coating}_{1313}/C^{matrix}_{1313}$, have been calculated. The results with spherical and prolate voids are displayed in Tables 4 and 5, respectively. It should be noted that, even with spherical voids, the overall behavior is still tetragonal due to the transversely isotropic nature of the PZT matrix. Since the coating is dielectrically softer than the PZT matrix, increasing the coating concentration will reduce the effective dielectric and piezoelectric constants, regardless of the condition whether coating is elastically stiffer or softer than the matrix. The variations of the effective stiffness however are closely tied to the ratio of coating to the matrix stiffness.

5.6. Periodic spherical inhomogeneities with eccentric, non-uniform thickness, coating

Our last calculation involves the unusual configuration of eccentric coating. In this case we consider a piezocomposite material consisting of PZT-7A spherical reinforcements with an eccentric spherical core inside each particle. Such a configuration with eccentricity of δ is shown in Fig. 7. Both inhomogeneity core and host matrix are assumed to possess non-piezoelectric isotropic behavior, but with the dielectric constants equal to five times the dielectric moduli of free space. Three different cases of eccentricity are considered, as below

$$\begin{aligned} &- \text{Case } 1 : \delta_1/\Lambda_1 = \delta_2/\Lambda_2 = \delta_3/\Lambda_3 = 0, \\ &- \text{Case } 2 : \delta_1/\Lambda_1 = \delta_2/\Lambda_2 = 0, \quad \delta_3/\Lambda_3 = 0.22, \\ &- \text{Case } 3 : \delta_1/\Lambda_1 = \delta_3/\Lambda_3 = 0, \quad \delta_2/\Lambda_2 = 0.22. \end{aligned} \tag{33}$$

Employing the present methodology, this set of problems has been solved for the volume fractions of $f^{core} = 4\%$ and $f^{coating} = 44\%$, and some selected values of shear moduli of coating layer and core. Since the coating layer is thick with variable thickness, it is subdivided into ten layers, which are all eccentric. The obtained effective properties are tabulated in Table 6. It is seen that the piezocomposite material still exhibits the overall tetragonal symmetry for cases 1 and 2, but for case 3 it is orthogonal.

Table 5a
Effective elastic properties of porous piezoelectric materials containing coated spheroidal voids, with $a_3/a_1 = 10$.

f^{void}	$f^{coating}$	$\frac{C^{coating}_{1313}}{C^{matrix}_{1313}}$	$\widetilde{C}_{1111}$	$\widetilde{C}_{1212}$	$\widetilde{C}_{1122}$	$\widetilde{C}_{3333}$	$\widetilde{C}_{1313}$	$\widetilde{C}_{1133}$
0.2	0	No coating	0.68	0.642	0.706	0.764	0.67	0.698
	0.04	0.5	0.653	0.62	0.681	0.753	0.656	0.671
		2.5	0.715	0.659	0.732	0.791	0.715	0.732
	0.08	0.5	0.643	0.603	0.663	0.738	0.621	0.65
		2.5	0.739	0.681	0.771	0.816	0.749	0.76
0.3	0	No coating	0.574	0.511	0.562	0.645	0.554	0.544
	0.06	0.5	0.513	0.493	0.528	0.587	0.520	0.510
		2.5	0.578	0.532	0.603	0.681	0.573	0.570
	0.12	0.5	0.481	0.478	0.494	0.539	0.496	0.463
		2.5	0.619	0.556	0.665	0.709	0.610	0.602

Table 5b
Effective piezoelectric and dielectric properties of porous piezoelectric materials containing coated spheroidal voids, $a_3/a_1 = 10$.

f^{void}	$f^{coating}$	$\frac{C^{coating}_{1313}}{C^{matrix}_{1313}}$	$\tilde{e}_{311}$	$\tilde{e}_{333}$	$\tilde{e}_{113}$	$\tilde{K}_{11}$	$\tilde{K}_{33}$
0.2	0	No coating	0.445	0.703	0.655	0.729	0.894
	0.04	0.5	0.429	0.674	0.63	0.685	0.803
		2.5	0.435	0.686	0.638	0.699	0.785
	0.08	0.5	0.412	0.659	0.608	0.63	0.746
		2.5	0.427	0.661	0.623	0.642	0.76
0.3	0	No coating	0.193	0.532	0.519	0.639	0.788
	0.06	0.5	0.178	0.506	0.483	0.596	0.731
		2.5	0.185	0.519	0.497	0.606	0.74
	0.12	0.5	0.163	0.481	0.457	0.481	0.665
		2.5	0.172	0.502	0.477	0.501	0.683

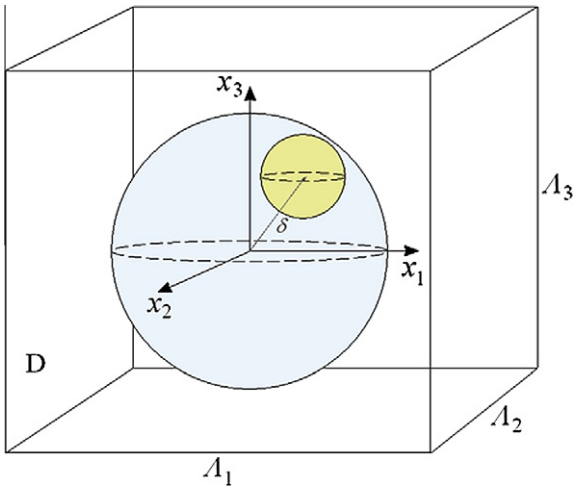

Fig. 7. A double-inhomogeneity system consisting of a PZT-7A spherical particle with an eccentric core in the RVE.

6. Concluding remarks

In this paper a new homogenization scheme has been developed to determine the effective electromechanical moduli of a piezoelectric composite containing periodic distribution of multi-coated inhomogeneities. To treat the multi-coated system, we have divided the nested inclusions into different regions, with each replaced by an equivalent inclusion that possesses certain amount of equivalent eigenstrain and electric field. Due to the periodic structure, the eigenfield is expanded in terms of the Fourier series. The local equivalent principle is then called upon, and integrated to give expressions for the average eigenstrain and electric field in terms of the applied external fields. Finally through the energy equivalence between a homogeneous effective medium and the heterogeneous one, the overall effective moduli are obtained in terms of the derived average eigenstrain-electric field for each phase. In this approach, the particle–matrix interactions and the inter-particle and intra-particle interactions are fully accounted for.

This newly developed scheme is quite robust. It can be applied to a wide range of complex systems where the coating does not have to be thin, the shape and orientation of the core and coatings do not have to be the same, the layout of the coated layers can be eccentric, the properties of each layer can be functionally graded, and the periodically distributed particles can be of the 2D elliptic or the 3D ellipsoidal shape. In this scheme the short-range interphase interactions, the particle–matrix interactions, and the long-range interactions between the periodically distributed inhomogeneities, have all been fully accounted for, so the theory is applicable to high volume concentration and high property contrast problems. It must be reminded that, in the computational process, a thick layer of coating must be subdivided into several layers to assure the numerical accuracy, the number of sub-layers to be determined from the convergent condition of the calculated results. While this subdivision process is somewhat cumbersome,

Table 6a
Effective elastic properties of piezocomposite consisting of eccentric spherical double-inhomogeneities for volume fractions of inhomogeneity core, $f^{core} = 0.04$ and its coating $f^{coating} = 0.44$.

δ/Λ	$\frac{C^{core}_{1313}}{C^{coating}_{1313}}$	$\frac{C^{matrix}_{1313}}{C^{coating}_{1313}}$	$\tilde{C}_{1111}$	$\tilde{C}_{1212}$	$\tilde{C}_{1122}$	$\tilde{C}_{3333}$	$\tilde{C}_{1313}$	$\tilde{C}_{1133}$	$\tilde{C}_{2222}$	$\tilde{C}_{2323}$	$\tilde{C}_{2233}$
$\delta_1/\Lambda_1 = 0$	0	0.5	0.367	0.415	0.274	0.359	0.446	0.308	0.367	0.446	0.308
$\delta_2/\Lambda_2 = 0$		2	1.167	1.210	1.084	1.189	1.923	1.066	1.167	1.923	1.066
$\delta_3/\Lambda_3 = 0$											
	2.5	0.5	0.470	0.538	0.373	0.481	0.626	0.405	0.470	0.626	0.405
		2	1.369	1.374	1.228	1.308	2.180	1.205	1.369	2.18	1.205
$\delta_1/\Lambda_1 = 0$	0	0.5	0.415	0.481	0.330	0.378	0.47	0.330	0.415	0.469	0.33
$\delta_2/\Lambda_2 = 0$		2	1.112	1.173	1.045	1.158	1.885	1.047	1.112	1.885	1.047
$\delta_3/\Lambda_3 = 0.22$											
	2.5	0.5	0.431	0.509	0.354	0.438	0.600	0.380	0.431	0.600	0.38
		2	1.405	1.440	1.282	1.348	2.225	1.265	1.405	2.225	1.265
$\delta_1/\Lambda_1 = 0$	0	0.5	0.396	0.457	0.309	0.370	0.458	0.319	0.404	0.466	0.325
$\delta_2/\Lambda_2 = 0.22$		2	1.130	1.200	1.060	1.172	1.909	1.058	1.119	1.188	1.051
$\delta_3/\Lambda_3 = 0$											
	2.5	0.5	0.455	0.527	0.363	0.450	0.612	0.399	0.448	0.604	0.385
		2	1.386	1.408	1.252	1.321	2.220	1.223	1.395	1.419	1.240

Table 6b
Effective piezoelectric and dielectric properties of piezocomposites made up eccentric spherical double-inhomogeneities for volume fractions of inhomogeneity core, $f^{core} = 0.04$ and its coating $f^{coating} = 0.44$.

δ/Λ	$\frac{C^{core}_{1313}}{C^{coating}_{1313}}$	$\frac{C^{matrix}_{1313}}{C^{coating}_{1313}}$	$\tilde{e}_{333}$	$\tilde{e}_{311}$	$\tilde{e}_{113}$	$\tilde{e}_{322}$	$\tilde{e}_{223}$	$\tilde{K}_{11}$	$\tilde{K}_{22}$	$\tilde{K}_{33}$
$\delta_1/\Lambda_1 = 0$	0	0.5	0.407	0.358	0.312	0.358	0.312	0.38	0.38	0.411
$\delta_2/\Lambda_2 = 0$		2	0.380	0.322	0.279	0.322	0.279	0.417	0.417	0.43
$\delta_3/\Lambda_3 = 0$										
	2.5	0.5	0.385	0.346	0.297	0.346	0.297	0.366	0.366	0.391
		2	0.359	0.309	0.256	0.309	0.256	0.394	0.394	0.415
$\delta_1/\Lambda_1 = 0$	0	0.5	0.421	0.371	0.329	0.371	0.329	0.412	0.412	0.427
$\delta_2/\Lambda_2 = 0$		2	0.405	0.340	0.291	0.340	0.291	0.435	0.435	0.451
$\delta_3/\Lambda_3 = 0.22$										
	2.5	0.5	0.402	0.359	0.311	0.359	0.311	0.385	0.385	0.418
		2	0.378	0.323	0.277	0.323	0.277	0.402	0.402	0.433
$\delta_1/\Lambda_1 = 0$	0	0.5	0.415	0.363	0.320	0.370	0.325	0.395	0.41	0.42
$\delta_2/\Lambda_2 = 0.22$		2	0.394	0.338	0.283	0.344	0.295	0.425	0.444	0.439
$\delta_3/\Lambda_3 = 0$										
	2.5	0.5	0.492	0.352	0.306	0.360	0.317	0.377	0.383	0.403
		2	0.364	0.316	0.269	0.327	0.273	0.402	0.416	0.425

it is – we believe – a small price to pay to solve this highly complex problem.

Acknowledgement

G.J. Weng was supported by the National Science Foundation, Mechanics of Materials Program, under CMS-0510409.

References

Barnett, D.M., Lothe, J., 1975. Dislocations and line charges in anisotropic piezoelectric insulators. Phys. Status Solidi B 67, 105–111.
Beckert, W., Kreher, W., Brau, W., Ante, M., 2001. Effective properties of composites fibers with a piezoelectric coating. J. Eur. Ceram. Soc. 21, 1455–1458.
Cherkaoui, M., Sabar, H., Berveiller, M., 1995. Elastic composites with coated reinforcements: a micromechanical approach for nonhomothetic topology. Int. J. Eng. Sci. 33, 829–843.
Christensen, R.M., Lo, K.H., 1979. Solutions for effective shear properties in three phase sphere and cylinder models. J. Mech. Phys. Solids 27, 315–330.
Dinzart, F., Sabar, H., 2009. Electroelastic behavior of piezoelectric composites with coated reinforcements: micromechanical approach and applications. Int. J. Solids Struct. 46, 3556–3564.
Dunn, M.L., Ledbetter, H., 1995. Elastic moduli of composites reinforced by multiphase particles. J. Appl. Mech. 62, 1023–1028.
Dunn, M.L., Taya, M., 1993. Micromechanics predictions of the effective electroelastic moduli of piezoelectric composite. Int. J. Solids Struct. 30, 161–175.
Eshelby, J.D., 1957. The determination of the elastic field of an ellipsoidal inclusion, and related problems. Proc. R. Soc. London A241, 376–396.
Fang, D.N., Jiang, B., Hwang, K.C., 2001. A modal for predicting effective properties of piezocomposites with non-piezoelectric inclusions. J. Elast. 62, 95–118.
Hill, R., 1983. Interfacial operators in the mechanics of composite media. J. Mech. Phys. Solids 31, 347–357.
Hori, M., Nemat-Nasser, S., 1993. Double-inclusion model and overall moduli of materials with microstructure. Mech. Mater. 14, 189–206.
Hori, M., Nemat-Nasser, S., 1994. Double-inclusion model and overall moduli of multi-phase composites. J. Eng. Mater. Tech. 116, 305–309.
Hu, G.K., Weng, G.J., 2000. The connections between the double-inclusion model and the Ponte Castaneda–Willis, Mori–Tanaka, and Kuster–Toksoz models. Mech. Mater. 32, 495–503.
Huang, J.H., 1995. Equivalent inclusion method for the work-hardening behavior of piezoelectric composites. Int. J. Solids Struct. 33, 1439–1451.
Jiang, C.P., Cheung, Y.K., 2001. An exact solution for the three-phase piezoelectric cylinder model under antiplane shear and its applications to piezoelectric composites. Int. J. Solids Struct. 38, 4777–4796.
Jiang, C.P., Tong, Z.H., Cheung, Y.K., 2001. A generalized self-consistent method for piezoelectric fiber reinforced composites under antiplane shear. Mech. Mater. 33, 295–308.
Li, J.Y., 2000. Magnetoelectroelastic multi-inclusion and inhomogeneity problems and their applications in composite materials. Int. J. Eng. Sci. 38, 1993–2011.
Li, C.Y., Weng, G.J., 2002a. Anti-plane crack problem in functionally graded piezoelectric materials. J. Appl. Mech. 69, 481–488.
Li, C.Y., Weng, G.J., 2002b. Yoffe-type moving crack in a functionally graded piezoelectric material. Proc. R. Soc. London A458, 381–399.
Lin, Y., Sodano, H.A., 2010. A double inclusion model for multiphase piezoelectric composites. Smart Mater. Struct. 19, 035003.
Mikata, Y., 2000. Determination of piezoelectric Eshelby tensor in transversely isotropic piezoelectric solids. Int. J. Eng. Sci. 38, 605–624.
Mori, T., Tanaka, K., 1973. Average stress in matrix and average elastic energy of materials with misfitting inclusions. Acta Metall. 21, 571–574.
Nemat-Nasser, S., Hori, M., 1999. Micromechanics: Overall Properties of Heterogeneous Materials. Elsevier, Amsterdam.
Nemat-Nasser, S., Yu, N., Hori, M., 1993. Bounds and estimates of overall moduli of composites with periodic microstructure. Mech. Mater. 15, 163–181.
Qiu, Y.P., Weng, G.J., 1991. Elastic moduli of thickly coated particle and fiber-reinforced composites. J. Appl. Mech. 58, 388–398.
Shen, M.H., Chen, S.N., Chen, F.M., 2005. Piezoelectric study on confocally multicoated elliptical inclusion. Int. J. Eng. Sci. 43, 1299–1312.
Sudak, L.J., 2003. Effect of an interphase layer on the electroelastic stresses within a three-phase elliptic inclusion. Int. J. Eng. Sci. 41, 1019–1039.
Wei, E.B., Poon, Y.M., Shin, F.G., Gu, G.Q., 2006. Effective properties of piezoelectric composites with periodic structure. Phys. Rev. B 74, 014107–014108.
Wu, T.L., 2000. Micromechanics determination of electroelastic properties of piezoelectric materials containing voids. Mat. Sci. Eng. A280, 320–327.
Yu, N., Somphone, T., 2009. The inclusion and inhomogeneity problems of electrostrictive materials with periodic microstructure. Mech. Mater. 41, 975–981.
Zhu, X., Xu, J., Meng, Z., 2000. Microdisplacement characteristics and microstructures of functionally gradient piezoelectric ceramic actuator. Mater. Des. 21, 561–566.